Chapter 4

Absolute Density Measures Estimation Functions with Very High Resolution Satellite Images

Ana Cristina Gonçalves and Adélia M. O. Sousa

Additional information is available at the end of the chapter

http://dx.doi.org/10.5772/intechopen.76817

Abstract

Assessment and monitoring of forest structure is frequently done with absolute density measures with field forest inventory data and expansion methods. The development of basal area and the number of trees estimation functions with data derived from very high spatial resolution satellite images enable their short-term and cost-effective evaluation, allowing also the estimation for the area not requiring extrapolation methods. The functions of basal area and the number of trees per hectare are based on crown cover obtained with very high spatial resolution satellite images for two evergreen oaks and umbrella pine. The three tree species are especially important in the agroforestry systems of the Mediterranean region. The linear functions fitted for pure stands of the three species and mixed stands of cork and holm oak and of cork oak and umbrella pine showed a better performance for basal area than for the number of trees per hectare. The inclusion of dummy variables for species composition improved the accuracy of the functions.

Keywords: quickBird image, multi-resolution segmentation, crown horizontal projection, absolute density measures, regression

1. Introduction

Holm oak (*Quercus rotundifolia*), cork oak (*Quercus suber*), and umbrella pine (*Pinus pinea*) are three of the most representative species in agroforestry systems in the Mediterranean basin [1, 2]. Their stands have usually low density, open heterogeneous canopies and as main production bark for cork oak and fruit for all [3–5]. They also have other productions, such as agricultural crops, pasture and extensive grazing. Due to the climate variability of the Mediterranean region, these multiple use systems enable risk dispersion and the sustainability in time [1, 2, 6].

Absolute density measures, especially the number of trees and basal area, are referred in silviculture textbooks as a proxy for competition and growing space at tree level and thus for growing conditions at stand level [7–15]. These measures are reported as a single value per stand, as the sum of the tree values, reported for a standard area, usually the hectare [7, 13, 16–19], and have the advantage of enabling comparison between different stands [7–15].

The conventional approach to calculate the number of trees and basal area is using field plots of forest inventories, which have a statistical sampling design and an expansion factor when working on an area basis [20–25]. Though a high accuracy is attained at field inventory plots, they have disadvantages related to the area sampled and the extrapolation methods needed for the evaluation on an area basis.

Remote sensing-derived data have been used to estimate both the number of trees [26–33] and basal area [26, 29, 30, 32, 34–40]. The advantages are the estimation for small and large areas [25, 41–43]; enabling time series analysis in short time cycles [25, 42]; data collection at different scales, depending on the imagery spatial resolution [42, 43]; and enabling the evaluation of the area not requiring extrapolation methods [44–49]. The disadvantages are related to the imagery spatial resolution; accuracy decreases with the increase of the pixel size [50–52].

2. Materials and methods

2.1. Satellite images and inventory data

Two satellite images were acquired as four-band products (Blue, Green, Red and Near-Infrared), with the bands pan-sharpened with the UNB algorithm [53]. The image from QuickBird satellite (hereafter Mora) was collected in August 2006, has an area of 80 km^2 (central coordinate 8°4′53.98″W and 38°51′16.12″N) and a spatial resolution of 0.7 m. The image from WorldView-2 satellite (hereafter Alcácer) was collected in June 2011, has an area of 35 km^2 (central coordinate 8°40′28.20″W and 38°27′45.71″N) and has a spatial resolution of 0.5 m. The forest area is composed of holm oak and cork oak in the former and cork oak and umbrella pine in the latter.

The images were orthorectified, georeferenced and atmospherically corrected. Ortho-rectification was carried out with the rational polynomial coefficient model (RCP) using the image metadata and ASTER GDEM digital elevation model (resolution 30 m) in Envi 4.8 [54]. For georeferencing the images, field data points obtained with global navigation satellite system (GNSS) were used, which resulted in a root mean square error (RMSE) of 0.49 m for Mora and 0.30 m for Alcácer. Atmospheric correction was done using the image digital number for top of atmosphere (ToA) reflectance to convert it to soil level reflectance using dark-object subtraction method [55].

From each image a vegetation mask per specie by a set of sequential steps was derived, using object-oriented analysis [56, 57]. Contrast split segmentation based on the normalized difference vegetation index image (NDVI, [58] in eCognition, version 8.0.1 [59]) was used to isolate tree crowns, resulting in a vegetation mask. In the second step multi-resolution segmentation

http://dx.doi.org/10.5772/intechopen.76817

[60] enabled the separation of the vegetation mask in different objects, using an algorithm with scale, shape and compactness as splitting parameters. The third step used the nearest neighbor algorithm to classify the objects per tree specie, in Weka 3.8.0 software [61], based on the descriptive statistics of the bands and on vegetation indices (NDVI, EVI, SAVI, and SR).

2.2. Inventory data

Each image was divided into a square grid, a function of their resolution, 65 × 65 pixels (45.5 × 45.5 m, 2070.25 m^2) for Mora and 90 × 90 pixels (45 × 45 m, 2025 m^2) for Alcácer. The grid area is similar to other studies with very high spatial resolution satellite images (e.g., [62]). Composition and crown cover (defined as the percent ratio between crown horizontal projection and grid area) were derived from the vegetation mask per specie using ArcGIS version 10 [63]. The grids were classified as monospecies if only one specie was present and multispecies otherwise. To design forest inventory, crown cover was grouped in three strata (10–30, 30–50 and >50%) and a random stratified sampling by proportional allocation was applied.

The field surveys took place in 2011 in Mora and 2013–2014 in Alcácer, measuring 17, 24 and 32 monospecies plots of holm oak (QR), cork oak (QS) and umbrella pine (PP), respectively, and 23 and 49 multispecies plots of holm oak and cork oak (QRQS) and cork oak and umbrella pine (QSPP), respectively. The total number of plots is 145. The main stand was defined as all individuals with diameter at breast height equal or larger than 6 cm for holm and cork oaks and 5 cm for umbrella pine. In each plot, for the main stand, diameter at breast height, total height and four crown radii (directions in north, south, east and west) were measured [16], as well as recorded tree location by GNSS. The number of trees per hectare (N) was defined as the sum of all individuals of the main stand per plot, scaled to a reference area, the hectare. Basal area per hectare (G) was defined as the sum of the sectional area of all the trees of the main stand in the plot, scaled to a reference area, the hectare [7, 16].

2.3. Statistical analysis

In the development of the functions for the number of trees and basal area per hectare, four types of functions were considered (**Figure 1**): (i) per composition classes (QR, QS, PP, QRQS and QSPP); (ii) not considering composition; (iii) considering crown cover per specie; and (iv) considering composition as dummy variables. Dummy variables were defined as a dichotomic variable where 1 refers to a specific composition (QR, QS, PP, QRQS or QSPP) and 0 to the other compositions. For (i) and (ii) the functions were fitted using ordinary least square linear regression through the origin (Eq. (1), where D is N or G, CC the crown cover and α the regression coefficient) and for (iii) and (iv) multiple linear regression with stepwise method and AIC as selection criteria (Eq. (2), where α and β are regression coefficients, d the dummy variables, i = QR, QS and PP and j = QR, QS, PP, QRQS and QSPP). For multiple regression, multicolinearity among explanatory variables was analyzed with the variance inflation factor (VIF), where no serious multicoliniarity is expected for VIF ≤ 10 [64, 65]. As suggested by several authors (e.g., [66, 67]) the sum of squares of the residuals (SQR), the coefficient of

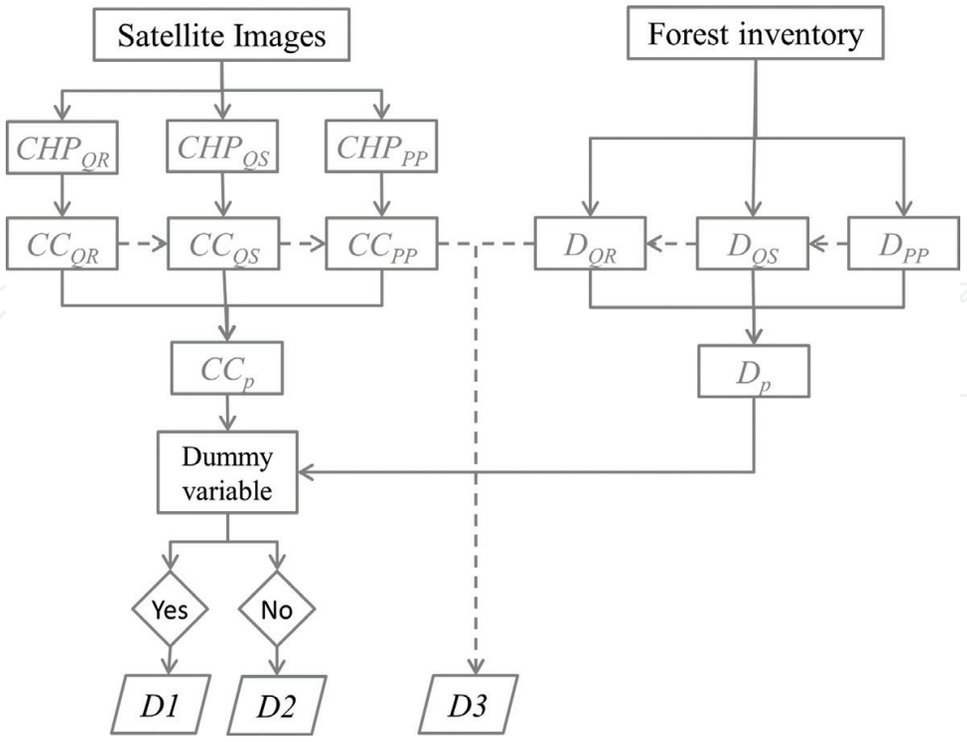

Figure 1. Model flow diagram (where *CHP* the crown horizontal projection in m², CC the crown cover, QR holm oak, QS cork oak, PP umbrella pine, and *p* the plot).

determination (R^2) and the adjusted coefficient of determination (R^2_{aj}) were used to evaluate the statistical properties of the models.

Whenever an independent data set is not available for model validation, re-sampling or jackknifing methods are recommended. One of these methods uses PRESS residuals, calculated as the difference between the observed and the estimated value of a variable (in this study N or G), as a cross-validation statistic [68–70], which is considered also to improve reliability in the accuracy assessment [43]. PRESS residuals are attained by fitting the model iteratively k times with n-1 observations (where n is the total number of observations) guaranteeing their independence [68–70]. The validation of the models was tested for bias and precision—the former with the mean of the PRESS residuals (Eq. (3), where PRESSrm is the mean of the PRESS residuals, y the observed value, ŷ the estimated value and i the number of the observation) and the latter with the mean of the absolute PRESS residuals values (PRESSram, Eq. (4)). To the former was added the analysis of the 5th and 95th percentile of the PRESS residuals [70]. Heteroscedasticity associated with the error term was evaluated graphically with the plots of the studentized residuals and the estimated values and the normality of the studentized residuals with normal quantile-quantile plots and Shapiro Wilk normality test, for a probability level of 0.001 [68, 71]. To enable comparison with other studies (e.g., [36]), the relative root mean square error (RMSEr, Eq. (5)) was also computed. The statistical analysis was done using R statistical software [72].

$$D = \alpha \times CC \tag{1}$$

http://dx.doi.org/10.5772/intechopen.76817

$$D = \alpha_i \times CC_i + \beta_j \times d_j \tag{2}$$

$$PRESS_{rm} = \frac{\sum_{i=1}^{n}\left(y_i - \hat{y}_{i,-1}\right)}{n} \tag{3}$$

$$PRESS_{ram} = \frac{\sum_{i=1}^{n}\left|y_i - \hat{y}_{i,-1}\right|}{n} \tag{4}$$

$$RMSE_r = \frac{\sqrt{\frac{\sum_{i=1}^{n}(y_i - \hat{y}_i)^2}{n}}}{\bar{y}} \times 100 \tag{5}$$

3. Results and discussion

3.1. Satellite image analysis

The vegetation mask per species accuracy resulting from the multi-resolution and object-oriented classification, illustrated in **Figure 2**, depends on several factors, namely the forest tree density, the limits between forest trees and other land uses, image date, forest tree species reflectance and crown shape. Stands with low density and isolated forest trees, such as holm oak, cork oak and umbrella pine in agroforestry systems, enable the distinction and separation of the tree crowns with accuracy in very high spatial resolution satellite images (e.g., [62]), minimizing the confounding effects of shadow pixels which occur in tree crowns at closer spacings [73]. Conversely, the diffused boundaries between forest tree crowns and other land uses can decrease classification accuracy [74]. Thus image dates with the highest contrast between different land uses, especially between herbaceous vegetation and forest trees, such as the summer (June–August) in the Mediterranean region, produce the smallest confounding influence [75, 76]. The other two variables that influence accuracy of the vegetation mask per species are the reflectance similarity between species and crown shapes, the more similar the lower the accuracy. The forest areas of Mora and Alcácer are composed predominantly of isolated trees, though some clusters occur, and the images were acquired in the dry summer period (June and August), thus with high contrast between the forest trees and the other land uses, especially the forest understory that was composed of soil and dry herbaceous vegetation. Regarding reflectance and crown shape, holm oak and cork oak have larger similarities with wide ranges of reflectance and an irregular crown shape when compared to umbrella pine that has a narrower reflectance range and nearly circular crowns. Nonetheless, the spectral signatures of the tree species are different enough to enable a good classification [44, 46–49]. The accuracy evaluated with Kappa statistic [77, 78] encountered true positives for 90% of the holm oak and 87% of the cork oak for Mora and 98% of the umbrella pine and 74% of the cork oak for Alcácer.

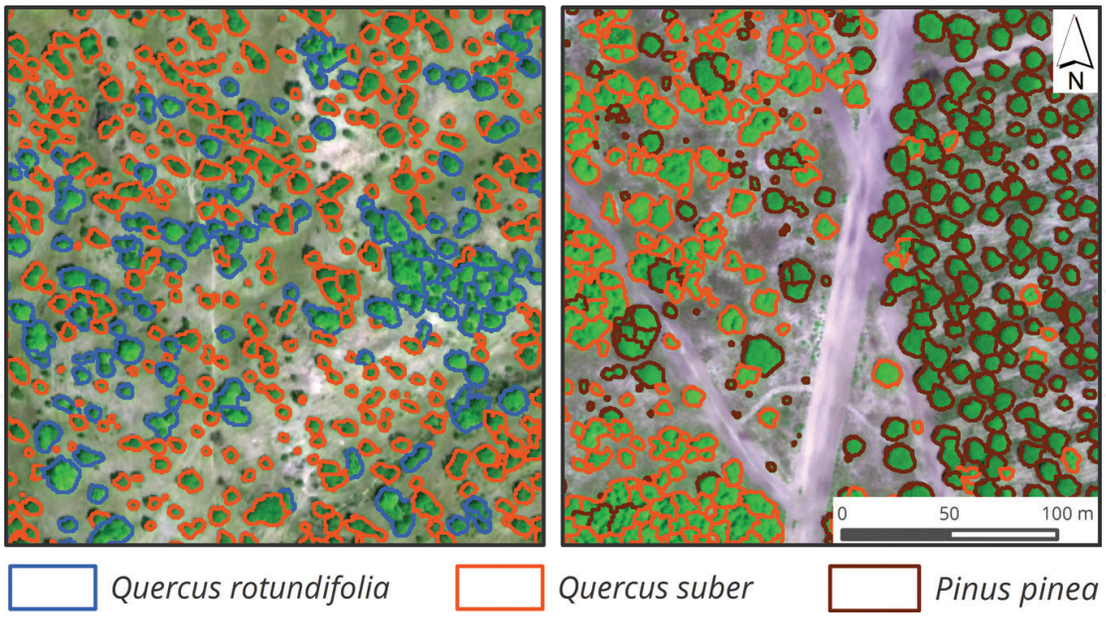

Figure 2. Illustration of vegetation mask for two small areas (left) Mora (cork and holm oak) and (right) Alcácer (cork oak and umbrella pine).

3.2. Number of trees and basal area functions

The variability for N is larger than for G and for QS, QRQS and QSPP than for QR and PP, denoted by the larger coefficient of variation (**Table 1** and **Figure 3**). The number of trees and their spatial distribution in the stand determine their growing space and the tree crown area is also a function of the species epinastic control [12] and spacing, with crown closure originating crown shyness [14], thus unbalancing the relation between crown cover and basal area and crown cover and number of trees. Holm oak, cork oak and umbrella pine have, especially in adult trees, weak epinastic control and are shade intolerant [5, 79], thus justifying the wide variability observed in the plots. However, positive correlations are observed for CC and G for all plots (0.72), stronger for QR (0.86) and QSPP (0.85) and weaker for QS and PP (0.66 each) and QRQS (0.62). These results are expected due to the almost direct relation between crown and stem diameters [80, 81]. Conversely, the correlation between CC and N is weaker when compared to the former. Positive correlations are found for all plots (0.47), stronger for QS (0.72), QR (0.57) and QSPP (0.54) and weaker for QRQS (0.36) and no correlation for PP (−0.04). The number of trees per hectare is frequently associated with the individual stems and the stage of development and the stand structure [7–15], giving rise to a higher variability in the number of trees (**Figure 4**).

In general, for the functions fitted for all composition classes (**Table 2**), there is an improvement in the statistical properties of the models from those not considering composition (N3 and G3) to those that included it as crown cover per specie (N2 and G2), with the best properties attained by those with composition as dummy variables (N1 and G1). For the number of trees, a reduction of −27.4% for SQR and an increase of 3.2% for R^2_{aj} from N3 to N1, a reduction of −18.0% for SQR and an increase of 2.1% for R^2_{aj} from N2 to N1 and a reduction

	Min	Max	Mean	SD	CV (%)	Min	Max	Mean	SD	CV (%)
	All					QR				
N	5	140	67	28.0	42.4	29	116	72	27	37.1
G (m^2 ha^{-1})	2.6	18.2	8.9	3.3	37.5	4.0	11.1	6.7	2.1	32.0
CC (%)	9.7	72.6	37.1	15.1	40.6	13.7	67.6	37.6	15.9	42.3
PHC (m^2)	195.8	1470.0	756.1	306.5	40.5	284.2	1399.0	777.7	329.2	42.3
	QS					PP				
N	5	135	60	33	54.2	5	119	72	23	32.4
G (m^2 ha^{-1})	5.2	15.4	9.1	2.8	30.7	3.8	15.9	9.5	2.6	27.5
CC (%)	13.4	70.5	35.3	14.0	39.7	13.0	66.7	40.5	17.1	42.3
PHC (m^2)	271.3	1460.2	723.9	293.0	40.5	263.5	1350.3	819.1	346.7	42.3
	QRQS					QSPP				
N	19	140	62	29	47.7	15	123	69	30	43.1
G (m^2 ha^{-1})	2.6	14.7	6.7	2.7	40.3	2.9	18.2	10.3	3.7	36.0
CC (%)	14.3	58.8	29.4	11.4	38.6	9.7	72.6	39.8	14.5	36.5
PHC (m^2)	296.9	1216.7	607.8	233.6	38.4	195.8	1470.0	804.9	293.9	36.5

Table 1. Descriptive statistics per composition classes (where N is the number of trees per hectare, G the basal area per hectare, CC the crown cover calculated with satellite data, PHC crown horizontal projection, max the maximum, min the minimum, SD the standard variation and CV the coefficient of variation).

of −8.0% for SQR and an increase of 1.0% for R^2_{aj} from N3 to N2 was observed. For basal area a reduction of −60.0% for SQR and an increase of 2.7% for R^2_{aj} from G3 to G1, a reduction of −53.5% for SQR and an increase of 2.5% for R^2_{aj} from G2 to G1 and a reduction of −4.3% for SQR and an increase of 0.2% for R^2_{aj} from G2 to G3 was observed. This is reflected in the better function performance of N1 or G1 when compared with N2 and N3 or G2 and G3. Bias is the lowest for N1 and G1 while precision is similar for all functions. The better statistical properties of N1 and G1 when compared with N3 and G3 could be, at least partially, explained by the inclusion of the composition variable in the functions as N and G have different behavior per composition classes (cf. **Table 2**). Comparing N1 and N2 or G1 and G2, the better performance of N1 and G1 can be explained by the relations between crown cover and the number of trees or basal area, for the different composition classes and probably by the influence of the clusters of mixed trees. When comparing N1 or G1, with the functions per composition class (Ni or Gi, i = 4,5,6,7,8), better model statistical properties are attained for N4 and N5 and G8 and G4, which correspond to the composition classes with smaller variability between CC and N and G (cf. **Table 2**), respectively. Nonetheless, in general, bias is larger for the number of trees than for the basal area. Similar results were attained for above-ground biomass functions with crown horizontal projection as an explanatory variable [44–46, 49]. The regression coefficients are presented in Eqs. (6)–(9) and **Table 3**.

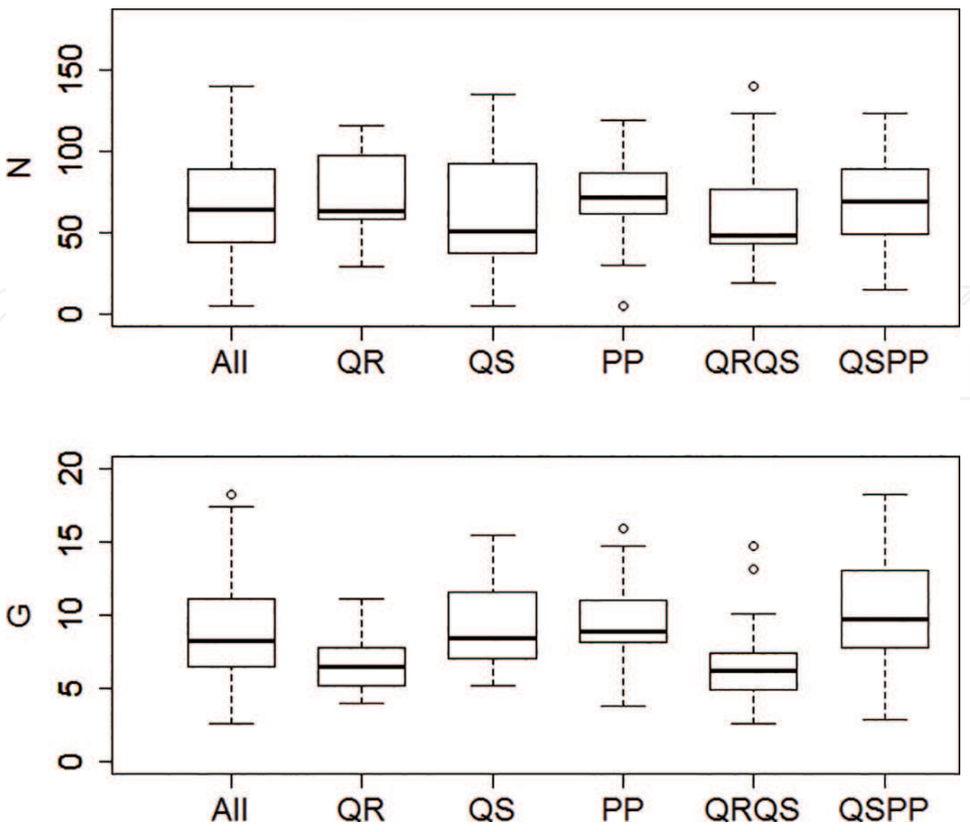

Figure 3. Boxplots of N and G for all plots and per composition class.

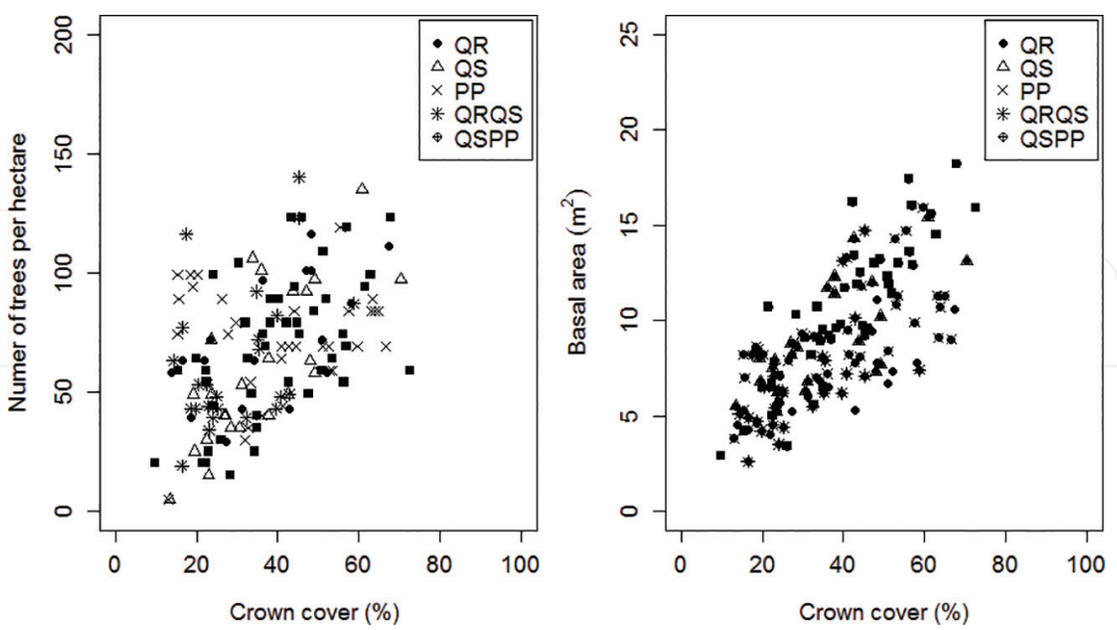

Figure 4. Crown cover and number of trees and basal area per composition class.

Model	Independent variables	SQR	R^2	R^2_{aj}	PRESSrm	PRESSram	Percentile		RMSEr
							5th	95th	
N									
N1	CC, dQR, dQS, dPP, dQRQS, dQSPP	89,148	0.884	0.879	0.002	0.828	−1.362	1.920	37.0
N2	CCQR, CCQS, CCPP	105,215	0.863	0.860	0.145	0.794	−1.178	1.966	40.1
N3	CC	113,595	0.852	0.851	0.172	0.802	−1.105	2.062	41.7
N4	CCQR	9870	0.900	0.893	0.196	0.912	−1.445	1.404	33.7
N5	CCQS	11,176	0.899	0.895	0.014	0.862	−1.146	1.873	35.9
N6	CCPP	37,293	0.795	0.788	0.300	0.776	−0.667	2.113	47.6
N7	CCQRQS	19,842	0.836	0.830	0.148	0.748	−1.303	1.873	44.6
N8	CCQSPP	31,382	0.878	0.875	0.111	0.833	−1.227	1.969	38.0
G									
G1	CC, dQR, dQS, dPP, dQRQS, dQSPP	585	0.955	0.953	0.001	0.794	−1.528	1.763	22.7
G2	CCQR, CCQS, CCPP	898	0.931	0.929	0.171	0.806	−1.690	1.729	28.1
G3	CC	936	0.928	0.927	0.162	0.810	−1.727	1.661	28.7
G4	CCQR	39	0.953	0.950	0.237	0.899	−1.301	1.602	22.8
G5	CCQS	142	0.935	0.932	0.202	0.883	−1.882	1.356	26.6
G6	CCPP	267	0.913	0.910	0.277	0.873	−1.304	1.627	30.5
G7	CCQRQS	136	0.898	0.894	0.136	0.805	−1.168	2.104	34.3
G8	CCQSPP	162	0.971	0.970	0.098	0.776	−1.432	1.654	18.1

Table 2. Statistical properties of the fitted functions (where CC is the crown cover, QR *Quercus rotundifolia*, QS *Querus suber*, PP Pinus pinea and d the dummy variable).

Model	α	Model	α
N3	1.68195	G3	0.22776
N4	1.7749	G4	0.16797
N5	1.7041	G5	0.2436
N6	1.5324	G6	0.21361
N7	1.9839	G7	0.21583
N8	1.65806	G8	0.255849

Table 3. Regression coefficients of the N and G functions.

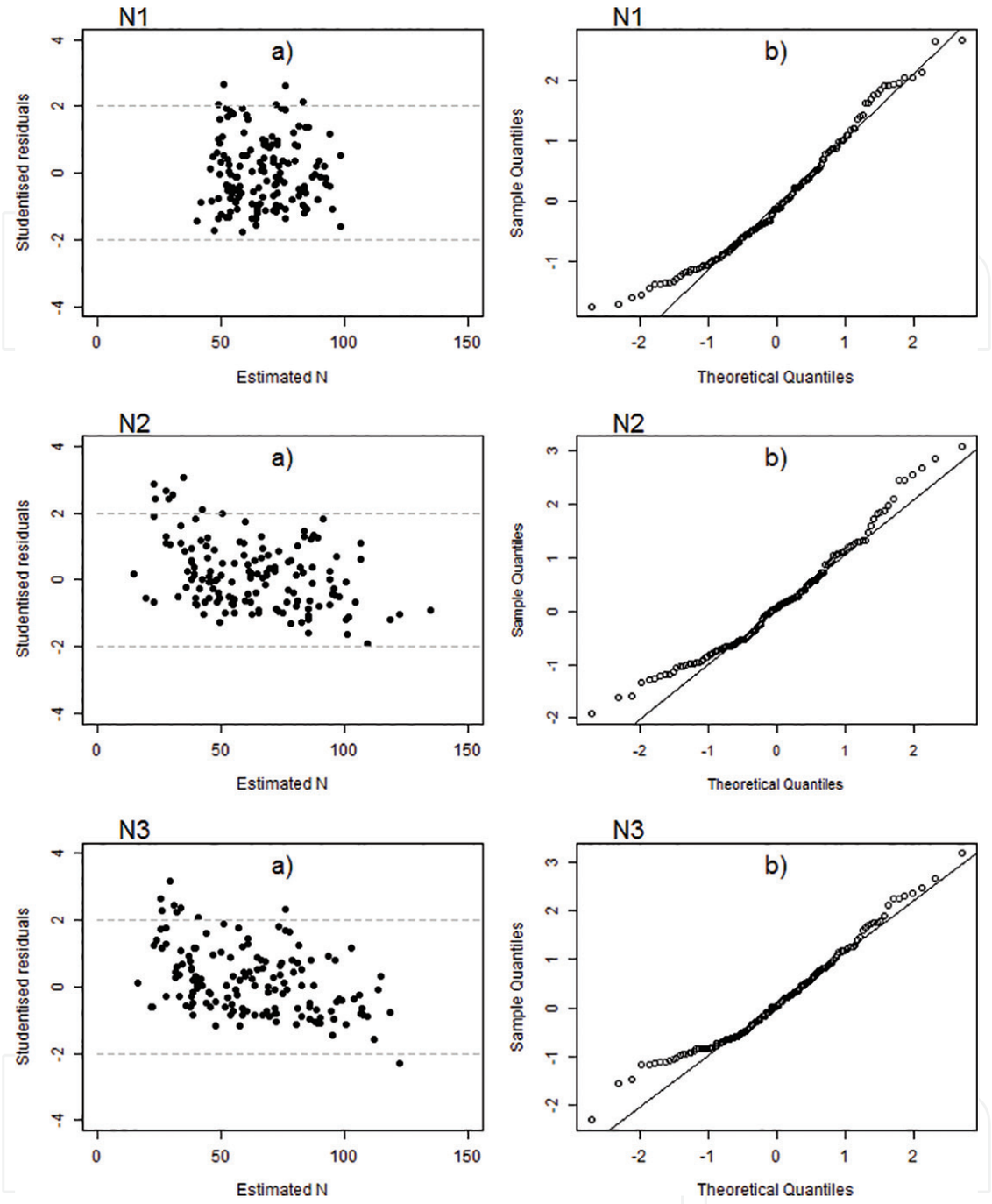

Figure 5. Studentized residuals (a) and normal probability (b) graphics for N1, N2, and N3.

$$N1 = 0.8982 \times CC + 37.7851 \times d_{QR} + 28.3933 \times d_{QS} + 35.4451 \times d_{PP} + 35.4373 \times d_{QRQS} + 33.1026 \times d_{QSPP} \quad (6)$$

$$N2 = 1.7334 \times CC_{QR} + 2.03536 \times CC_{QS} + 1.50642 \times CC_{PP} \quad (7)$$

http://dx.doi.org/10.5772/intechopen.76817

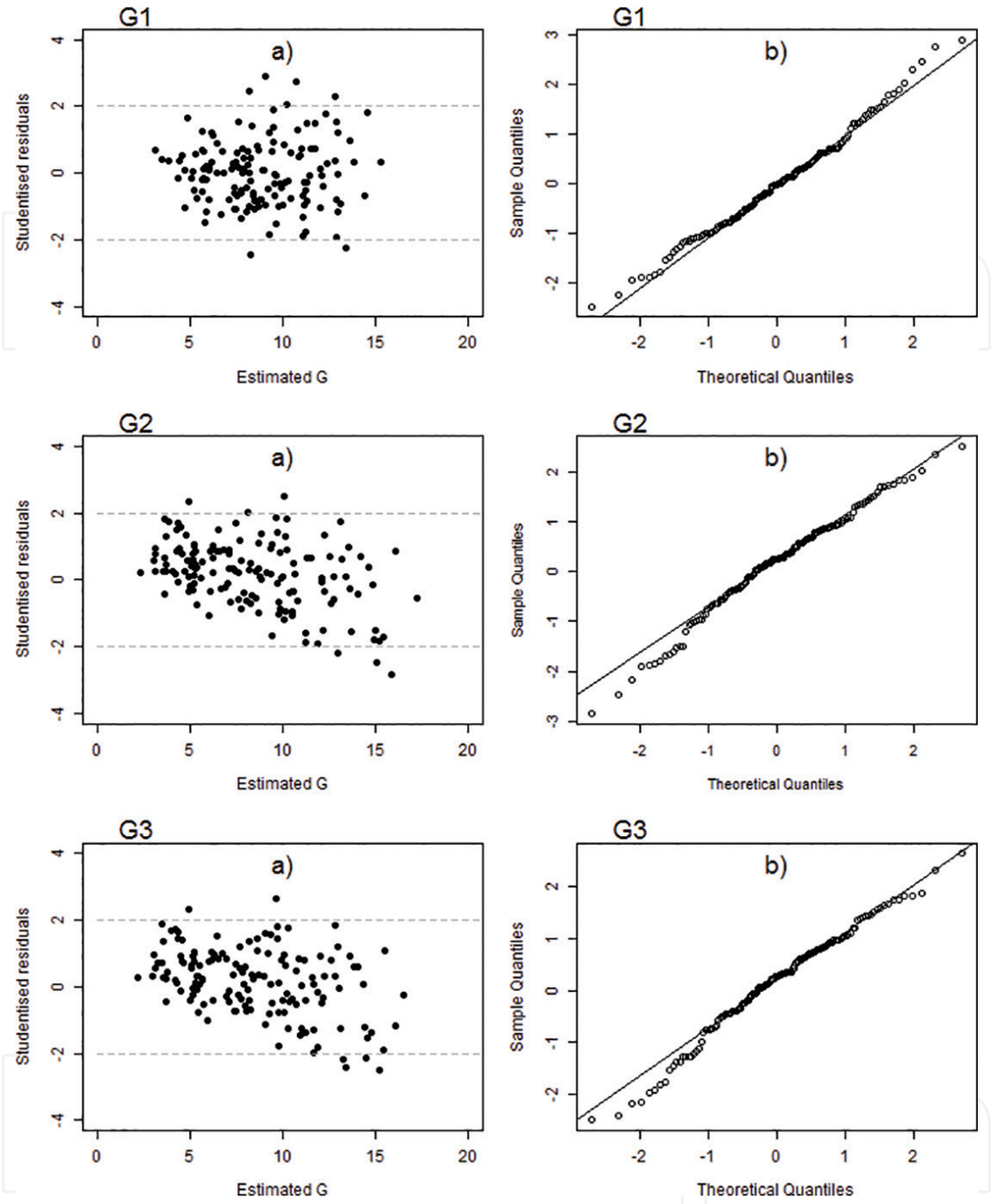

Figure 6. Studentized residuals (a) and normal probability (b) graphics for G1, G2, and G3.

$$G1 = 0.14992 \times CC + 1.04399 \times d_{QR} + 3.84375 \times d_{QS} + 3.39116 \times d_{PP} + 2.25474 \times d_{QRQS} + 4.37992 \times d_{QSPP} \quad (8)$$

$$G2 = 0.19954 \times CC_{QR} + 0.2234 \times CC_{QS} + 0.237722 \times CC_{PP} \quad (9)$$

The coefficient of determination of the functions to estimate the number of trees per hectare with explanatory variables derived from satellite data is rather variable from 0.38 to 0.88 [26, 29, 30, 32]; an even wider variation is found for the functions to estimate the basal area per hectare, from 0.07 to 0.92 [26, 29, 30, 32, 35, 40]. In general, the functions for N and G estimation developed in this study have higher R^2 than those of the aforementioned studies. RMSEr decreases from N3 and G3 to N1 and G1 (**Table 2**) and is smaller than that attained value for the basal area as studied by reference Hyvönen et al. [36] (46–53%) and Günlü et al. [40] (29–34%).

For N1, N2, G1 and G2, no serious multicoliniarity is expected as VIF for all explanatory variables is smaller than 7.7. The studentized residuals of N1, N2, N3, G1, G2 and G3 do not show systematic variations; the normal probability graphs approach the straight line (**Figures 5** and **6**), thought with deviations in the extremes, which is corroborated by the residuals not meeting normality (all, $p < 0.001$). Similar results were attained for N3–N8 and G4–G8.

4. Conclusions

The vegetation mask per species from very high-resolution satellite images enables deriving accurately crown cover. In spite of the similarities between holm oak, cork oak and umbrella pine, the methods of multi-segmentation and object-oriented classification allow their distinction with accuracy.

The functions with the best performances for the number of trees per hectare and basal area per hectare for the three species were attained with the explanatory variable crown cover and composition classes as dummy variables.

The agroforestry systems in general, and those of holm oak, cork oak and umbrella pine in particular, have high spatial variability which makes these functions well suited to evaluate and monitor their stands in space and time.

Acknowledgements

The authors would like to thank all the forest producers for permission to undertake forest inventory; Paulo Mesquita for image processing; and Carla Coelho, David Gomes and Pedro Antunes for their fieldwork. The work was financed by Programa Operativo de Cooperação Transfronteiriço Espanha–Portugal (POCTEP), project Altercexa–Medidas de Adaptación y Mitigación del Cambio Climático a Través del Impulso de las Energías Alternativas en Centro, Alentejo y Extremadura (Refª 0317_Altercexa_I_4_E and 0406_ALTERCEXA_II_4_E), TrustEE–innovative market based Trust for Energy Efficiency investments in industry (Project ID: H2020–696140) and National Funds through FCT–Foundation for Science and Technology under the Project UID/AGR/00115/2013.

Conflict of interest

Both authors declare that there is no conflict of interest.

Author details

Ana Cristina Gonçalves* and Adélia M. O. Sousa

*Address all correspondence to: acag@uevora.pt

Department of Rural Engineering, School of Sciences and Technology, Institute of Mediterranean Agricultural and Environmental Sciences (ICAAM), Institute of Research and Advanced Information (IIFA), University of Évora, Évora, Portugal

References

[1] Nerlich K, Graeff-Hönninger S, Claupein W. Agroforestry in Europe: A review of the disappearance of traditional systems and development of modern agroforestry practices, with emphasis on experiences in Germany. Agroforestry Systems. 2013;**87**:475-492

[2] Eichhorn MP, Paris P, Herzog F, Incoll LD, Liagre F, Mantzanas K, Mayus M, Moreno G, Papanastasis VP, Pilbeam DJ, Pisanelli A, Dupraz C. Silvoarable systems in Europe—Past, present and future prospects. Agroforestry Systems. 2006;**67**:29-50

[3] Gonçalves AC. Multi-species stand classification: Definition and perspectives. In: Chakravarty S, Shukla G, editors. Forest Ecology and Conservation. Rijeka: INTECH; 2017. pp. 4-23

[4] Gonçalves AC, Afonso A, Pereira DG, Pinheiro A. Influence of umbrella pine (*Pinus pinea* L.) stand type and tree characteristics on cone production. Agroforestry Systems. 2017a;**91**:1019-1030

[5] Correia AV, Oliveira AC. Principais espécies florestais com interesse para Portugal: zonas de influência mediterrânica. [Main forest species with interest for Portugal: Zones of Mediterranean influence]. Lisboa: Direcção-Geral das Florestas. Estudos e Informação, 1999. p. 318

[6] Jose S, Gillespie AR, Pallardy SG. Interspecific interactions in temperate agroforestry. Agroforestry Systems. 2004;**61**:237-255

[7] Assmann E, editor. The Principles of Forest Yield Study. Oxford: Pergamon Press; 1970. p. 506

[8] Boudru M. Forêt et Sylviculture. Le traitement des forêts [Forest and Silviculture. The Treatment of Forests]. Tome 2. Gembloux: Presses Agronomiques de Gembloux; 1989. p. 344. [in French]

[9] Matthews JD. Silvicultural Systems. Oxford: Claredon Press; 1989. p. 284

[10] Lanier L, Badré M, Delabraze P, Dubourdieu J, Flammarion JP. Précis de sylviculture [Compendium of Silviculture]. Nancy: ENGREF; 1986. p. 468. [in French]

[11] Schütz JP. Sylviculture 1. Principes d'éducation des forêts [Silviculture 1. Principals of Tending Forests]. Lausanne: Presses Polytechniques et Universitaires Romandes; 1990. p. 245. [in French]

[12] Oliver CD, Larson BC. Editors. Forest Stand Dynamics. Update Editions. New York: John Wiley & sons, Inc; 1996. p. 544

[13] Smith DM, Larson BC, Kelty MJ, Ashton PMS. The Practice of Silviculture. Applied Forest Ecology. 9th ed. New York: John Wiley & Sons, Inc; 1997. p. 560

[14] Schütz JP. Sylviculture 2. La gestion des forêts irrégulières et mélangées. Collection Gérer L'environement, n° 13. Lausanne: Presses Polytechniques et Universitaires Romandes; 1997. p. 178. [in French]

[15] O'Hara KL. Multiaged Silviculture: Managing for Complex Forest Stand Structures. Oxford: Oxford University Press; 2014. p. 213

[16] Avery TE, Burkhart HE, editors. Forest Measurements. 4th ed. New York: Macgraw-Hill Inc; 1994. p. 480

[17] Philip MS. Measuring Trees and Forests. 2nd ed. Cambridge: CAB International; 1994. p. 310

[18] Av L, Akça A, editors. Forest Msensuration. Sringer. Dordrecht: Sringer; 2009. p. 383

[19] West PW. Tree and Forest Measurement. 2nd ed. Dordrecht: Sringer; 2009. p. 190

[20] Brown S, Gillespie AJR, Lugo AE. Biomass estimation methods for tropical forests with applications to forest inventory data. Forest Science. 1989;**35**:881-902

[21] Gillespie AJR, Brown S, Lugo AE. Tropical forest biomass estimation from truncated stand tables. Forest Ecology and Management. 1992;**48**:69-87

[22] Houghton RA, Lawrence KT, Hackler JL, Brown S. The spatial distribution of forest biomass in the Brazilian Amazon: A comparison of estimates. Global Change Biology. 2001;**7**:731-746

[23] Tomppo E, Haakana M, Katila M, Peräsaari J. Multi-Source National Forest Inventory—Methods and Applications. Managing Forest Ecosystems 18. Dordrecht: Springer Science+ Business Media; 2008. p. 373

[24] Vidal C, Lanz A, Tomppo E, Schadauer K, Gschwantner T, di Cosmo L, Robert N. Establishing forest inventory reference definitions for forest and growing stock: A study towards common reporting. Silva Fennica. 2008;**42**(2):247-266

[25] McRoberts R, Tomppo E, Naesset E. Advanced and emerging issues on national forest inventories. Scandinavian Journal of Forest Research. 2010;**25**:368-381

[26] Hudak AT, Crookston NL, Evans JS, Falkowski MJ, Smith AM, Gessler PE, Morgan P. Regression modeling and mapping of coniferous forest basal area and tree density from discrete-return LiDAR and multispectral satellite data. Canadian Journal of Remote Sensing. 2006;**32**:126-138

[27] Hirata Y, Tabuchi R, Patanaponpaiboon P, Pougparn S, Yoneda R, Fujioka Y. Estimation of aboveground biomass in mangrove forest using high-resolution satellite data. Journal of Forest Research. 2014;**19**:34-41

[28] Sedano F, Goméz D, Gong P, Biging G. Tree density estimation in a tropical woodland ecosystem with multiangular MISR an MODIS data. Remote Sensing of Environment. 2008;**112**:2523-2537

[29] Kayitakire F, Hamel C, Defourny P. Retrieving forest structure variables based on image texture analysis and IKONOS-2 imagery. Remote Sensing of Environment. 2006; **102**:390-401

[30] Özdemir I, Karnieli A. Predicting forest structural parameters using the image texture derived from WorldView-2 multispectral imagery in a dryland forest, Israel. International Journal of Applied Earth Observation and Geoinformation. 2011;**13**(5):701-710

[31] Mohammadi J, Joibary SS, Yaghmaee F, Mahiny AS. Modeling forest stand volume and tree density using Landsat ETM + data. International Journal of Remote Sensing. 2010;**31**(11):2959-2975

[32] Gómez C, Wulder MA, Montes F, Delgado JA. Modelling forest structural parameters in Mediterranean pines of Central Spain using QuickBird-2 imagery and classification and regression tree analysis (CART). Remote Sensing. 2012;**4**(1):135-159

[33] Kahriman A, Günlü A, Karahalil U. Estimation of crown closure and tree density using landsat TM satellite images in mixed forest stands. Journal of Indian Society of Remote Sensing. 2014;**42**(3):559-567

[34] Meng Q, Cieszewski C, Madden M. Large area forest inventory using Landsat ETM+: A geostatistical approach. ISPRS Journal of Photogrammetry and Remote Sensing. 2009;**64**:27-36

[35] Hyyppä J, Hyyppä H, Inkinen M, Engdahl M, Linko S, Zhu Y-H. Accuracy comparison of various remote sensing data sources in the retrieval of forest stand attributes. Forest Ecology and Management. 2000;**128**:109-120

[36] Hyvönen P, Pekkarinen A, Tuominen S. Segment-level stand inventory for forest management. Scandinavian Journal of Forest Research. 2005;**20**(1):75-84

[37] Poulain M, Peña M, Schmidt A, Schmidt H, Schulte A. Relationships between forest variables and remote sensing data in a Nothofagus pumilio forest. Geocarto International. 2010;**25**:25-43

[38] Gebreslasie MT, Ahmed FB, van Aardt JAN. Predicting forest structural attributes using ancillary data and ASTER satellite data. International Journal of Applied Earth Observation and Geoinformation 2010;**12**:S23-S26

[39] Jung M, Tautenhahn S, Wirth C, Kattge J. Estimating basal area of spruce and fir in post-fire residual stands in Central Siberia using Quickbird, feature selection, and random forests. Procedia Computer Science. 2013;**18**:2386-2395

[40] Günlü A, Ercanlı I, Sönmez T, Başkent EZ. Prediction of some stand parameters using pan-sharpened IKONOS satellite image. European Journal of Remote Sensing. 2014;**47**(1):329-342

[41] Greenberg JA, Dobrowski SZ, Ustion SL. Shadow allometry: Estimating tree structural parameters using hyperspatial image analysis. Remote Sensing of Environment. 2005;**97**:15-25

[42] Eisfelder C, Kuenzer C, Dech S. Derivation of biomass information for semi-arid areas using remote-sensing data. International Journal of Remote Sensing. 2012;**33**(9):2937-2984

[43] Lu D, Chen Q, Wang G, Liu L, Li G, Moran EA. A survey of remote sensing-based aboveground biomass estimation methods in forest ecosystems. International Journal of Digital Earth. 2016;**9**(1):63-105

[44] Sousa AMO, Gonçalves AC, Mesquita P, Marques da Silva JR. Biomass estimation with high resolution satellite images: A case study of *Quercus rotunifolia*. ISPRS Journal of Photogrametric and Remote Sensing. 2015;**101**:69-79

[45] Gonçalves AC, Sousa AMO, Mesquita PG. Estimation and dynamics of above ground biomass with very high resolution satellite images in *Pinus pinaster* stands. Biomass and Bioenergy. 2017b;**106**:146-154

[46] Gonçalves AC, Sousa AMO, Silva JRM. Pinus pinea above ground biomass estimation with very high spatial resolution satellite images. In: Carraquinho I, Correia AC, Mutke S, editors. Mediterraneanpine Nuts From Forest and Plantations. Vol. 122. Options Mediterranées. 2017. pp. 49-54

[47] Macedo FL, Sousa AMO, Gonçalves AC, Silva HR, Rodrigues RAF. Estimativa do volume de madeira para *Eucalyptus* sp. com imagens de satélite de alta resolução espacial. Scientia Forestalis. 2017;**45**(114):237-247

[48] Malico I, Gonçalves AC, Sousa AMO. Assessment of the availability of forest biomass for biofuels production in Southwestern Portugal. In: Defect and Diffusion Forum. Vol. 371. 2017. pp. 121-127

[49] Sousa AMO, Gonçalves AC, Silva JRM. Above ground biomass estimation with high spatial resolution satellite images. In: Tumuluru JS, editor. Biomass Volume Estimation and Valorization for Energy. Rijeka: InTech; 2017. pp. 47-70

[50] Xie Y, Sha Z, Yu M. Remote sensing imagery in vegetation mapping: A review. Journal of Plant Ecology. 2008;**1**:9-23

[51] Boyle SA, Kennedy CM, Torres J, Colman K, Pérez-Estigarribia PE, de la Sancha NU. High-resolution satellite imagery is an important yet underutilized resource in conservation biology. PLoS One. 2014;**9**(1):e86908

[52] As-syakur RA, Osawa T, Adnyana IWS. Medium spatial resolution satellite imagery to estimate gross primary production in an urban area. Remote Sensing. 2010;**2**:1496-1507

[53] Zhang Y, Mishra RK. From UNB PanSharp to Fuze go—The success behind the pan-sharpening algorithm. International Journal of Image Data Fusion. 2013;**5**:39-53

[54] Envi. Reference Guide—Exelis Visual Information Solutions. Boulder, Colorado: Exelis Visual Information Solutions [Internet]. 2009. Available from: http://www.exelisvis.com/portals/0/pdfs/envi/envi_zoom_user_guide.pdf [Accessed: November 27, 2012]

[55] Chavez PS Jr. An improved dark-object subtraction technique for atmospheric scattering correction of multispectral data. Remote Sensing of Environment. 1988;**24**(3):459-479

[56] Blaschke T. Object based image analysis for remote sensing. ISPRS Journal of Photogrammetry & Remote Sensing. 2010;**65**:2-16

[57] Blaschke T, Hay GJ, Kelly M, Lang S, Hofmann P, Addink E, Queiroz Feitosa R, van der Meer F, van der Werff H, van Coillie F, Tiede D. Geographic object-based image analysis—Towards a new paradigm. ISPRS Journal of Photogrammetry & Remote Sensing. 2014;**87**:180-191

[58] Rouse JW, Haas RH, Schell JA, Deering DW. Monitoring vegetation systems in the Great Plains with ERTS. In: 3rd ERTS Symposium, NASA; 1973. SP-351 I. pp. 309-317

[59] Definiens Imaging. eCognition Developer 8.0.1 Reference Book [Internet]. 2010. Available from: http://www.definiens.com [Accessed: October 23, 2012]

[60] Baatz M, Schäpe A. Multiresolution segmentation: an optimization approach for high quality multi-scale image segmentation. In: Angew. Geogr. Informationsverarbeitung XII. Beiträge zum Agit. Salzbg. Karlsruhe: Herbert Wichmann Verlag; 2000. pp. 12-23

[61] Eibe F, Hall MA, Witten IH. The WEKA Workbench. Online Appendix for Data Mining: Practical Machine Learning Tools and Techniques. 4th ed. Cambridge (USA): Morgan Kaufmann; http://www.cs.waikato.ac.nz/ml/weka/Witten_et_al_2016_appendix.pdf

[62] Ozdemir I. Estimating stem volume by tree crown area and tree shadow area extracted from pan# sharpened Quickbird imagery in open Crimean juniper forests. International Journal of Remote Sensing. 2008;**29**(19):5643-5655

[63] Esri. ArcGIS Desktop: Release 10. Redlands, CA: Environmental Systems Research Institute [Internet]. 2010. Available from: http://www.esri.com [Accessed: January 23, 2013]

[64] Legendre P, Legendre L, editors. Numerical Ecology. 3th ed. Vol. 24. Amsterdam: Elsevier Science BV; 2012. p. 1006

[65] Sheather SJ, editor. A Modern Approach to Regression with R. New York: Springer Texts in Statistics; 2009. p. 393

[66] Burkhart HE, Tomé M, editors. Modelling Forest Trees and Stands. Dordrecht: Springer Science+Business Media; 2012. p. 457

[67] Pretzsch H, editor. Forest Dynamics, Growth and Yield: From Measurement to Model. Berlin Heidelberg: Springer-Verlag; 2009. p. 664

[68] Myers RH, editor. Classical and Modern Regression with Applications. Chicago: Duxbury Press; 1986. p. 488

[69] Clutter JL, Fortson JC, Pienaar LV, Briester GH, Bailey RL, editors. Timber Managment: A Quantitative Approach. New York: John Wiley & Sons, Inc; 1983. p. 333

[70] Paulo JA, Palma JHN, Gomes AA, Faias SP, Tomé J, Tomé M. Predicting site index from climate and soil variables for cork oak (*Quercus suber* L.) stands in Portugal. New Forests. 2015;**46**:293-307

[71] Montgomery DC, Peck EA. Introduction to Linear Regression Analysis. New York: Wiley; 1982

[72] R Development Core Team. R: A language and environment for statistical computing. R Foundation for Statistical Computing [Internet]. 2017. Available from: http://www.R-project.org [Accessed: December 06, 2017]

[73] Ke Y, Quackenbush LJ. A review of methods for automatic individual tree-crown detection and delineation from passive remote sensing. International Journal of Remote Sensing. 2011;**32**(17):4725-4747

[74] Massada AB, Kent R, Blank L, Perevolotsky A, Hadar L, Carmel Y. Automated segmentation of vegetation structure units in a Mediterranean landscape. International Journal of Remote Sensing. 2012;**33**(2):346-364

[75] Nguyen HC, Jung J, Lee J, Choi S-U, Hong S-Y, Heo J. Optimal atmospheric correlation for above-ground forest biomass estimation with the ETM+ remote sensor. Sensors. 2015;**15**:18865-18886

[76] Wu W, De Pauw E, Helldén U. Assessing woody biomass in African tropical savannahs by multiscale remote sensing. International Journal Remote Sensing. 2013;**34**(13):4525-4549

[77] Stehman SV. Estimating the kappa coefficient and its variance under stratified random sampling. Photogrammetric Engineering & Remote Sensing. 1996;**62**:401-407

[78] Congalton RG, Oderwald RG, Mead RA. Assessing Landsat classification accuracy using discrete multivariate statistical techniques. Photogrammetric Engineering and Remote Sensing. 1983;**49**:1671-1678

[79] Mutke S, Calama R, González-Martínez SC, Montero G, Gordo J, Bono D, Gil L. Mediterranean stone pine: Botany and horticulture. Horticultural Reviews. 2012;**39**: 153-201

[80] Hemery GE, Savill PS, Pryor SN. Applications of the crown diameter–stem diameter relationship for different species of broadleaved trees. Forest Ecology and Management. 2005;**215**:285-294

[81] Verma NK, Lamb DW, Reid N, Wilson B. An allometric model for estimating DBH of isolated and clustered eucalyptus trees from measurements of crown projection area. Forest Ecology and Management. 2014;**326**:125-132